

# Atomic Force Microscopy Study of Hydroxypropylcellulose Films Prepared from Liquid Crystalline Aqueous Solutions

M. H. Godinho,<sup>\*,†</sup> J. G. Fonseca,<sup>‡</sup> A. C. Ribeiro,<sup>‡,§</sup> L. V. Melo,<sup>§</sup> and P. Brogueira<sup>§,||</sup>

Dept. Ciência dos Materiais and CENIMAT, Faculdade de Ciências e Tecnologia, Universidade Nova de Lisboa, 2829-516 Caparica, Portugal; Centro de Física da Matéria Condensada, Universidade de Lisboa, 1649-003 Lisboa Portugal; Dept. de Física, Instituto Superior Técnico, 1049-001 Lisboa, Portugal; and ICEMS, Instituto Superior Técnico, 1049-001 Lisboa, Portugal

Received October 29, 2001

**ABSTRACT:** We have shown in this work that a tunable topographical system can be obtained from aqueous hydroxypropylcellulose (HPC) liquid crystalline solutions. The HPC solid films were prepared by casting isotropic and liquid crystalline solutions under shear. Atomic force microscopy (AFM) measurements of their topographical features were performed. The features of the film surface can be affined by controlling the processing conditions. We have demonstrated that the films prepared from liquid crystalline solutions (HPC/water ratio: 50–65% w/w) show two periodic structures, primary and secondary set. The former consists of the bands perpendicular to the shear direction while the latter has the bands slightly tilted from that direction. An out-of-plane angle variation (9°–13°), of the sinusoidal molecular orientation, is also reported. A fractal analysis of these surfaces indicates a scale-invariant nature between 300 nm and 4  $\mu\text{m}$ .

## Introduction

The formation of banded textures in thin-film samples of solutions of liquid crystalline polymers (LCP), subjected to shear, has been reported in the literature since 1979.<sup>1</sup> Fundamental research on these systems is particularly active,<sup>2</sup> due to a large number of physical interactions involved.<sup>3</sup> Moreover, the surface anisotropy of the mechanical and optical properties of the polymer films,<sup>4</sup> together with their potential use as alignment layers for liquid crystal displays,<sup>5</sup> makes these systems particularly interesting and promising for new applications. At present, the main challenge is the possibility of fine-tuning of surface topography and structure by modifying some experimental parameters.

Because of the symmetry properties of the liquid crystal solutions, large domains of well-oriented polymer chains are formed during the shear flow, while the defects are squeezed into small regions. The shear accounts for an additional energy stored in the solution. When the shear is stopped, the system will first relax with a characteristic time  $t_b$  to a transient state. In this state the distortion energy is minimized, and the orientational order is kept, resulting in a banded structure. This behavior is observed only if two conditions are fulfilled:<sup>6</sup> (a) if the shear rate,  $\dot{\gamma}$ , is higher than a critical shear rate,  $\dot{\gamma}^c$ , with  $\dot{\gamma}^c$  being strongly dependent on the molecular weight,  $M$ , of the polymer and slightly sensitive to the polymer concentration,  $C$ , according to the relation<sup>7</sup>

$$\dot{\gamma}^c \propto C^{-1} M^{-7} \log M \quad (1)$$

and (b) if the shearing time,  $t_s$ , is longer than a critical time that depends on the shear rate. This means that

there is a minimum deformation,  $\gamma^c$ , below which the periodic structure was not observed. The general dependency of the band formation time,  $t_b$ , on the experimental parameters is known<sup>7</sup> (e.g., in the first approximation  $t_b \sim t_s^{-2}$ ,  $t_b$  increases with the molecular weight  $M$ ), but no analytical expression was yet deduced, due to the complexity of the dynamic behavior of LCPs under shear.

The band structure may be characterized by the band spacing (typically 4–10  $\mu\text{m}$ )<sup>8</sup> that, in contrast with some theoretical predictions,<sup>9</sup> seems to be independent of the film thickness. Some previously described experiments<sup>10</sup> indicate that the band spacing is relatively insensitive to the shear rate, while different authors<sup>10,11</sup> reported conflicting results concerning the effect of the polymer concentration.

The band microstructure is energetically very stable, but it only persists during a characteristic time  $t_d$  (typically  $t_d \sim 10$  min). The thermal agitation may be sufficient for the system to overcome the energy barrier between the band texture (local minimum) and the nondistorted state (overall minimum). The bands begin to lose their parallel orientation; they form elongated domains and finally collapse, giving rise to an equilibrium state. As expected, the time  $t_d$  is found to be strongly dependent<sup>6</sup> on the molecular weight ( $t_d$  increases with  $M$ ) and on the shear rate ( $t_d$  increases with  $\dot{\gamma}$ ).

The hydroxypropylcellulose (HPC) aqueous lyotropic solutions are, regarding the ability to form band texture, among the most studied systems described in the literature.<sup>7,12</sup> The formed periodic structures can be locked within the polymer after the solvent evaporation, if the evaporation time is shorter than the relaxation time  $t_d$ .

Atomic force microscopy (AFM) data, as reported in the literature, indicate that the films obtained from HPC in acetic acid<sup>13</sup> show a molecular “serpentine” trajectory, with an out-of-plane component, that was associated with the band texture. But this particular

<sup>†</sup> Universidade Nova de Lisboa.

<sup>‡</sup> Universidade de Lisboa.

<sup>§</sup> Dept. de Física, Instituto Superior Técnico.

<sup>||</sup> ICEMS, Instituto Superior Técnico.

\* Author for correspondence: e-mail mhg@fct.unl.pt.

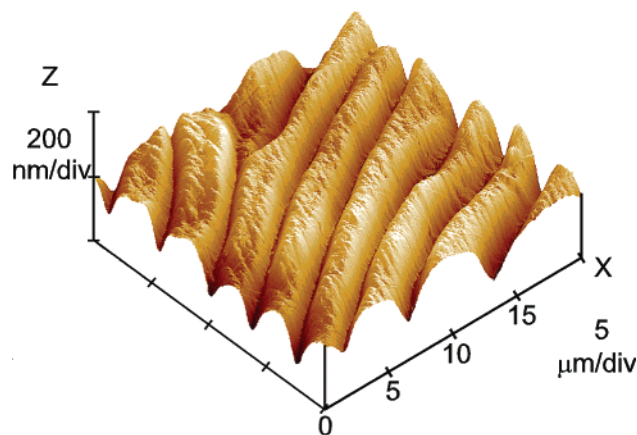


**Figure 1.** 3D topography image ( $20 \times 20 \mu\text{m}^2$  scan) of the free surface of a sheared HPC film prepared from a 60% w/w solution at a shear rate  $v_1 = 5 \text{ mm/s}$ .

behavior could be associated with the possible chemical reaction of the acetic acid with the HPC hydroxyl groups. The esterification reaction was already reported for cellulose derivatives in the presence of trifluoroacetic acid.<sup>11</sup> Thin films obtained from HPC/water liquid crystalline solutions were also reported in the literature, showing a leveling of the fibrillar topology that was attributed<sup>15</sup> to the long time required for drying of the films.

In this work we report the use of AFM to perform quantitative measurements of topographical features of HPC solid films prepared from different concentrations of HPC/water solutions and two shear rates.

### Experimental Section

Five solutions of HPC (Aldrich 100 000 molecular weight) in water (HPC/water: 30% w/w; 50% w/w; 55% w/w; 60% w/w; 65% w/w) were prepared at room temperature followed by centrifugation to remove air bubbles. The films were casted and sheared simultaneously by moving a casting knife at two controlled shear rates:  $v_1 = 5 \text{ mm/s}$  and  $v_2 = 10 \text{ mm/s}$ . The thickness of the dried films was measured using a Mitutoyo digital micrometer, with a range from 14 to  $30 \mu\text{m}$ . A D3100 with a Nanoscope IIIa controller from Digital Instruments (DI) was used for the AFM. The measurements were performed in

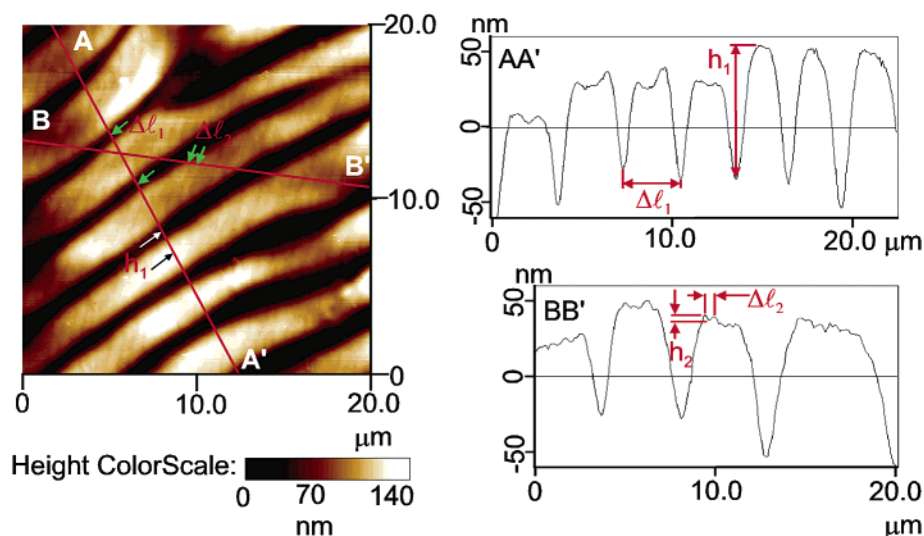
tapping mode under ambient conditions. A commercial tapping mode etched silicon probe from DI and a  $90 \times 90 \mu\text{m}^2$  scanner were used. Images consisted of raster scanned, electronic renderings of sample surfaces.

### Results and Discussion

Figure 1 shows the 3D topography image ( $20 \times 20 \mu\text{m}^2$  scan) of the free surface of a sheared HPC film prepared from a 60% w/w solution at a shear rate  $v_1 = 5 \text{ mm/s}$ . The image shows two different scale ranges: a primary set of "large" bands, perpendicular to the shear direction, and a smoother texture characterized by a secondary periodic structure containing "small" bands.

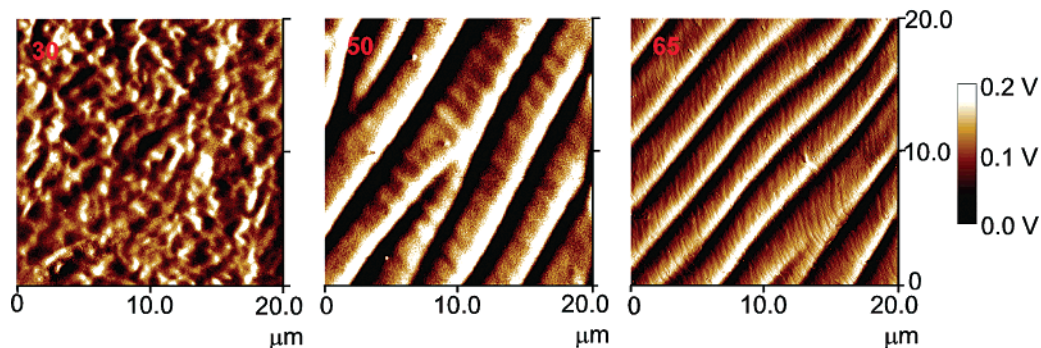
Figure 2 shows a top view image of the height scan of the surface shown in Figure 1 and the analysis of the height profile at two cross sections: AA' and BB'. Cross section AA' was taken along the shear direction. The periodicity of the "large" bands,  $\Delta l_1$ , and the average peak-to-valley height for these bands,  $h_1$ , were determined from the AA' height profile plot, as indicated. Cross section BB' was taken along the direction of the secondary periodic "small" bands. The periodicity of the "small" bands,  $\Delta l_2$ , and their peak-to-valley height,  $h_2$ , were measured from the BB' height profile plot, as indicated. The arrows on the top of the view image along AA' and BB' lines mark the points used for the measurements performed in the height profile plots.

Figure 3 shows the top view image of the amplitude scan of the free surface of three sheared HPC films prepared at a shear rate of  $v_1 = 5 \text{ mm/s}$  from solutions of different concentrations: (a) 30% w/w, (b) 50% w/w, and (c) 65% w/w. The surface of the film prepared from 30% w/w does not possess any periodicity. A primary and a secondary set of bands were observed only on the films prepared from anisotropic solutions, i.e., 50–65% w/w. Moreover, the films prepared from the solutions of the same concentration, using a higher shear rate ( $v_2 = 10 \text{ mm/s}$ ), exhibit similar topographies, but they are characterized by different parameters. At a constant concentration, for example at 65% w/w, the periodicity of the bands ( $\Delta l_1$ ) shows a tendency to decrease when the shear rate increases ( $\Delta l_1(v_1) = 2.97 \mu\text{m}$  and  $\Delta l_1(v_2) = 1.97 \mu\text{m}$ ). At a constant shear rate, as the concentration of the polymer increases, the periodicity of the



**Figure 2.** Top view image of the height scan of the surface shown in Figure 1 and the height profile analysis at the two cross sections: AA' and BB'. The arrows on the top of a view image along AA' and BB' lines mark the points used for the measurements of the height profile.





**Figure 3.** Top view image of the amplitude scan of the free surface of three sheared HPC films prepared at a shear rate of  $v_1 = 5$  mm/s from solutions with HPC/water ratios: (a) 30% w/w, (b) 50% w/w, and (c) 65% w/w.

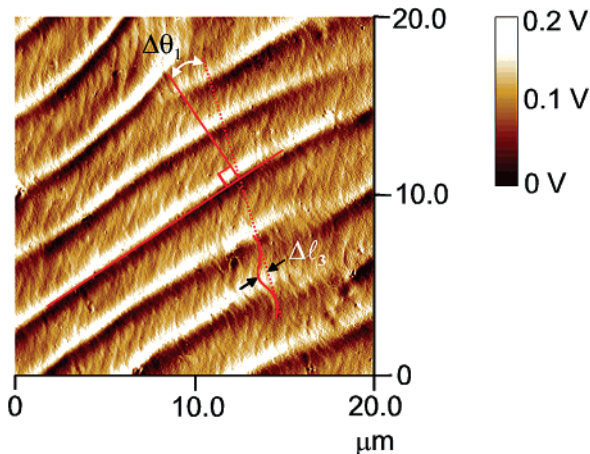


**Figure 4.** Top view image of the amplitude scan of the surface shown in Figure 1. The secondary set of bands is at angle  $\Delta\theta_1$  to the shear direction. The horizontal distance between the line that joins both valley coordinates of a secondary band and the point obtained from the projection of the peak of the same secondary band on the horizontal plane,  $\Delta l_3$ , is used to calculate the out-of-plane angle of the sinusoidal variation in the molecular orientation,  $\theta_P$ .

bands decreases (for  $v_1$ , at 50% w/w and 65% w/w,  $\Delta l_1 = 4.68 \mu\text{m}$  and  $\Delta l_1 = 2.97 \mu\text{m}$ , respectively). The analysis of the AFM height profile perpendicular to the shear direction shows an average peak-to-valley height of  $h_1 = 70\text{--}100$  nm for these bands, and it is independent of solution concentration or shear rate. The bands of secondary periodicity show a tendency to decrease with the increase of polymer concentration ( $\Delta l_2(v_1) = 1.52 \mu\text{m}$  for 50% w/w and  $\Delta l_2(v_1) = 0.493 \mu\text{m}$  for 65% w/w). The AFM height profile along the shear direction gives an average peak-to-valley height of  $h_2 = 2\text{--}5$  nm. The secondary set of bands appears at an angle  $\Delta\theta_1$  to the shear direction (Figure 4). The angle  $\Delta\theta_1$  tends to increase when the concentration of the polymer increases ( $\Delta\theta_1(v_1) = 8^\circ$  for 50% w/w and  $\Delta\theta_1(v_1) = 26^\circ$  for 65% w/w). We have also found that the sinusoidal variation of the molecular orientation does not occur in the plane of shear but makes an out-of-plane angle,  $\theta_P$ . This angle was calculated from the relation

$$\theta_P = \arctan\left(\frac{h_1}{\Delta l_3}\right) \quad (2)$$

where  $\Delta l_3$  is the horizontal distance between the line that joins the valley coordinates of a secondary band and the point obtained from the projection of the peak of that particular secondary band on the horizontal

plane. Typically,  $\Delta l_3$  is determined from the top view image as indicated in Figure 4. It was found that the angle  $\theta_P$  varies from  $9^\circ$  to  $13^\circ$  and shows a tendency to decrease when the concentration of polymer in the precursor solution decreases. No clear dependence on the shear rate was observed.

The presence of the out-of-plane component was reported in the literature<sup>13</sup> and was estimated to be in the range of  $4\text{--}10^\circ$  for a  $20 \mu\text{m}$  thick film prepared from a 37% w/w solution of HPC in acetic acid. It was thought that the contractional strain induced by stress relaxation was responsible for the observed effect.<sup>13</sup>

The free surface topography of sheared HPC films prepared from solutions of different polymer concentration exhibits distinct behavior for different shear rates. For solutions of the high polymer concentration (HPC/water > 55% w/w) the topography is characterized by two periodic sets of bands for both shear rates: a primary set, perpendicular to the shear direction, showing a decreasing periodicity with increasing shear rate, and a secondary set, having a decreasing periodicity when polymer content increases. These films do not show dependence on the shear rate. For the solution of low polymer concentration (HPC/water  $\leq 55\%$  w/w) the increase of the shear rate seems to prevent the formation of the band structure. For solutions with concentrations of HPC below 50% w/w, no bands were observed for neither shear rate. At 50% w/w solution concentration the band structure is clearly observable in films prepared with the low shear rate ( $v_1 = 5$  mm/s) but is not detectable for the high shear rate ( $v_2 = 10$  mm/s). Figure 5 represents a 3D image of the free surface topography of two sheared films prepared with 55% w/w at two shear rates. It can be seen from the figure that the band structure is well-defined for this solution concentration at both shear rates. The increase of the shear rate promotes a slight irregularity on the film surface, instead of causing decrease of the primary band periodicity, as observed on films prepared from higher solution concentrations. The results obtained for films prepared from solutions of different concentration of HPC and different shear rates are summarized and compared in Table 1.

To further characterize these surfaces, a fractal analyses may prove to be useful, since it can be used to describe irregular surfaces and contribute to a better understanding of their properties.<sup>16</sup> The roughness of surfaces may be scale-invariant in a particular scale range, and in these cases the fractal dimension,  $D_f$ ,<sup>17</sup> may be used to describe the film surface topography.

We measure the fractal dimension using the variance method and dividing the full AFM images into equal-

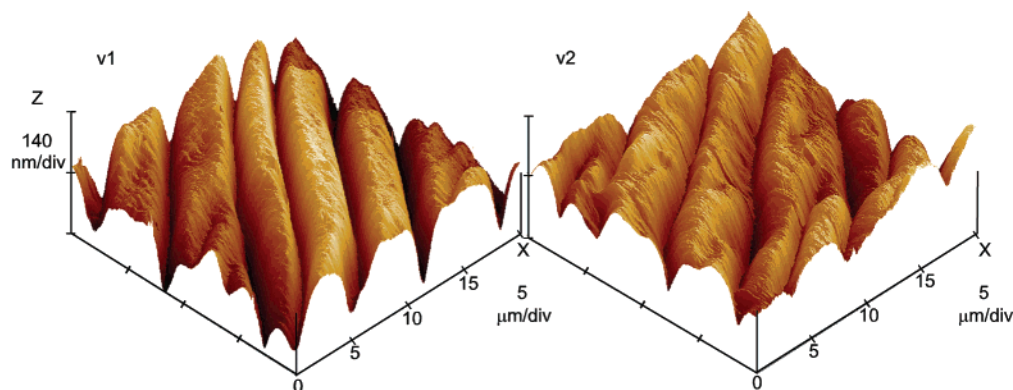


**Figure 5.** 3D images of the free surface topography of two sheared films prepared from a HPC/water ratio of 55% w/w at two shear rates:  $v_1 = 5$  mm/s and  $v_2 = 10$  mm/s.

**Table 1. Results Obtained for Films Prepared from Solutions of Different Concentration of HPC and Different Shear Rates<sup>a</sup>**

solution concn (w/w)	shear rate (mm/s)	$\Delta l_1$ ( $\mu\text{m}$ )	$h_1$ (nm)	$\Delta l_2$ ( $\mu\text{m}$ )	$h_2$ (nm)	$\Delta\theta_1$ (deg)	$\theta_P$ (deg)	film thickness ( $\mu\text{m}$ )
50	5	4.3–5.2	84–89	1.42–1.80	4.5–9.1	$\approx 8$		14
50	10							21
55	5	3.1–4.3	87–96	0.72–1.80	3.5–9.0	$< 14$		14
55	10	3.5–4.1	80–90	0.75–1.0	3.43	10 (?)		18
60	5	2.9–3.2	71–98	0.55–0.67	4.4–5.0	30	9–10	22
60	10	1.9–2.9	72–80	0.35–0.55	2.1–4.7	18	12	28
65	5	2.9–3.3	80–100	0.44–0.59	4.8	26	15	19
65	10	1.8–2.1	74–87	0.35–0.40	2.9–4.4	23–28	13	30

<sup>a</sup>  $\Delta l_1$  is the periodicity of the “large” bands, and the average peak-to-valley height for these bands is  $h_1$ . The periodicity of the secondary “small” bands is  $\Delta l_2$  and their peak-to-valley height,  $h_2$ . This secondary set of bands appears at an angle  $\Delta\theta_1$  to the shear, and their sinusoidal variation of the molecular orientation does not occur in the plane of shear but makes an out-of-plane angle,  $\theta_P$ .

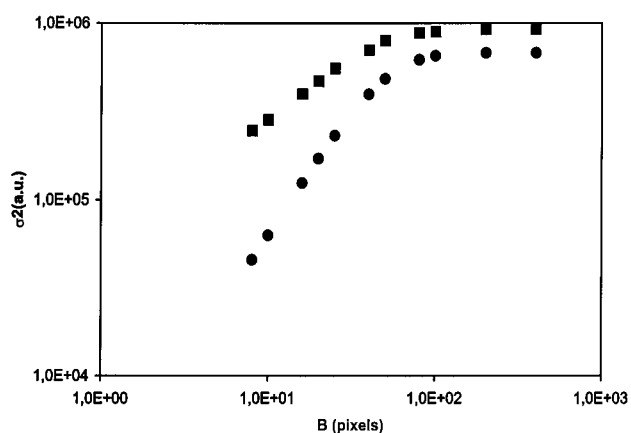


**Figure 6.** Plot of the variance  $\sigma^2$  as a function of the box size  $B$  (from 20  $\mu\text{m}$  square images with 512 pixels) for the case of thin films prepared from a solution with  $C = 55\%$  HPC in water and two different shear rates (circles,  $v_1 = 5$  mm/s; squares,  $v_2 = 10$  mm/s). The linear behavior indicates a self-affine nature of the film surface between 300 nm and 4  $\mu\text{m}$ .

size squared boxes. The variance  $\sigma^2$  is, for a particular box size, given by the relation

$$\sigma^2(B) = \left\langle \frac{1}{B^2 - 1} \sum_{i=1}^{B^2} (z_i - \bar{z})^2 \right\rangle \quad (3)$$

where  $B^2$  is the total number of data points in the box,  $z_i$  is the height in each point,  $\bar{z}$  is the average height in a box, and  $\langle \dots \rangle$  denotes averaging over all nonoverlapping boxes covering the total image. The variance  $\sigma^2$  increases with the box size  $B$ :

$$\sigma^2 \propto B^{2(3-D_f)} - (2\Delta)^{2(3-D_f)} \quad (4)$$

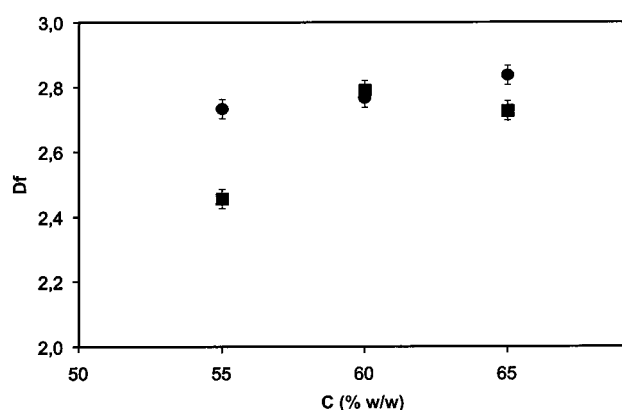


**Figure 7.** Fractal dimension,  $D_f$ , as a function of the polymer concentration,  $C$ , at two different shear rates: circles,  $v_1 = 5$  mm/s; squares,  $v_2 = 10$  mm/s. In general, the fractal dimension increases with both the polymer concentration and the shear rate.

where  $\Delta$  is the instrumental resolution, in this case, the distance between data points. When  $D_f$  is not extremely high, the last term in eq 4 can be neglected, and the fractal dimension  $D_f$  is directly determined from the linear fit of the plot  $\log \sigma^2$  vs  $\log B$  ( $=62.4\pi/q$ ). Figure 6 shows the variance  $\sigma^2$  vs the box size  $B$  for a solid film made from the 55% w/w solution at two different shear rates (circles,  $v_1 = 5$  mm/s and squares,  $v_2 = 10$  mm/s). The linear behavior for  $B$  smaller than 100 pixels indicates a self-affine nature of the film surface.

We have determined  $D_f$ , eq 4, for different concentrations of polymer and different shear rates (Figure 7). It was found that the HPC films are self-affined between 300 nm and 4  $\mu\text{m}$ . In this range, the fractal dimension shows a tendency to increase with both the polymer

concentration and the shear rate. This fact is in good agreement with the observed dependency of the banded structure on these two parameters.

The surfaces are not self-affine for higher dimensions.

## Conclusions

A tunable topographic system may be obtained from HPC aqueous liquid crystalline solutions. The results point out that two kinds of periodicities may be locked and adjusted in these systems as a function of the processing conditions. The films are found to be self-affine between 300 nm and 4  $\mu\text{m}$  but not for higher scales. In general, the fractal dimension is found to increase with both polymer concentration and shear rate. This trend reflects the increasing complexity of the surface topography when the films are prepared with higher polymer concentrations or with higher shear rates.

**Acknowledgment.** This work was supported by Project POCTI/32597/CTM/2000-FEDER and by the Portuguese Science Foundation (FCT) through Pluri-annual contracts with CENIMAT and ICEMS. J. G. Fonseca also gratefully acknowledges FCT for Grant BPD/5633/2001.

## References and Notes

- (1) Aharoni, S. M. *Macromolecules* **1979**, *12*, 271–280.
- (2) See for example: Mather, P. T.; Jeon, H. G.; Han, C. D.; Chang, S. *Macromolecules* **2000**, *33*, 7594–7608.
- (3) Israelachvili, J. N. *Intermolecular and Surface Forces*; Academic Press: London, 1985.
- (4) Wang, J.; Labes, M. M. *Macromolecules* **1992**, *25*, 5790–5793.
- (5) Wang, J.; Bhattacharya, S.; Labes, M. *Macromolecules* **1991**, *24*, 4942–4947.
- (6) Marsano, E.; Carpaneto, L.; Ciferri, A. *Mol. Cryst. Liq. Cryst.* **1988**, *153*, 267–278.
- (7) Ernst, B.; Navard, P. *Macromolecules* **1989**, *22*, 1419–1422.
- (8) Viney, C.; Putnam, W. *Polymer* **1995**, *36*, 1731–1741.
- (9) Zielinska, B. J. A.; Bosch, A. *Phys. Lett. A* **1988**, *38*, 5465–5468.
- (10) Fincher, C. R. *Mol. Cryst. Liq. Cryst.* **1988**, *155*, 559–570.
- (11) Donald, A. M.; Viney, C.; Ritter, A. P. *Liq. Cryst.* **1986**, *1*, 287–300.
- (12) Riti, J. B.; Cidade, M. T.; Godinho, M. H.; Martins, A. F.; Navard, P. *J. Rheol.* **1997**, *41*, 1247–1259.
- (13) Patnaik, S.; Bunning, T.; Adams, W.; Wang, J.; Labes, M. *Macromolecules* **1995**, *28*, 393–395.
- (14) Ritcey, A. M.; Holme, K. R.; Gray, D. G. *Macromolecules* **1988**, *21*, 2914–2917.
- (15) Mori, N.; Morimoto, M.; Nakamura, K. *Macromolecules* **1999**, *32*, 1488–1492.
- (16) Bunde, A.; Havlin, S. *Fractals and Disordered Systems*; Springer: Sitio, 1996.
- (17) Rao, M. V. H.; Mathur, B. K.; Chopra, K. L. *Appl. Phys. Lett.* **1994**, *65*, 124–126.
- (18) Almqvist, N. *Surf. Sci.* **1996**, *355*, 221–228.

MA0118769